

# One novel quinoxaline derivative as a potent human cyclophilin A inhibitor shows highly inhibitory activity against mouse spleen cell proliferation

Jian Li,<sup>a,†</sup> Jing Chen,<sup>a,†</sup> Li Zhang,<sup>a,†</sup> Feng Wang,<sup>a</sup> Chunshan Gui,<sup>a</sup> Li Zhang,<sup>c</sup>  
Yu Qin,<sup>c</sup> Qiang Xu,<sup>c</sup> Hong Liu,<sup>a</sup> Fajun Nan,<sup>a</sup> Jingkan Shen,<sup>a</sup> Donglu Bai,<sup>a</sup>  
Kaixian Chen,<sup>a</sup> Xu Shen<sup>a,b,\*</sup> and Hualiang Jiang<sup>a,b,\*</sup>

<sup>a</sup>Drug Discovery and Design Centre, State Key Laboratory of Drug Research, Shanghai Institute of Materia Medica, Shanghai Institutes for Biological Sciences, Chinese Academy of Sciences, Shanghai 201203, China

<sup>b</sup>School of Pharmacy, East China University of Science and Technology, Shanghai 200237, China

<sup>c</sup>State Key Laboratory of Pharmaceutical Biotechnology, School of Life Sciences, Nanjing University, 22 Han Kou Road, Nanjing 210093, China

Received 10 March 2006; revised 21 April 2006; accepted 21 April 2006

Available online 6 May 2006

**Abstract**—Cyclophilin A (CypA) is a ubiquitous cellular enzyme playing critical roles in many biological processes, and its inhibitor has been reported to have potential immunosuppressive activity. In this work, we reported a novel quinoxaline derivative, 2,3-di(furan-2-yl)-6-(3-*N*,*N*-diethylcarbamoyl-piperidino)carbonylamino quinoxaline (DC838, **3**), which was confirmed to be a potent inhibitor against human CypA. By using the surface plasmon resonance (SPR) and fluorescence titration techniques, the kinetic analysis of CypA/DC838 interaction was quantitatively performed. CypA peptidyl prolyl *cis*–*trans* isomerase (PPIase) activity inhibition assay showed that DC838 demonstrated highly CypA PPIase inhibitory activity. In vivo assay results showed that DC838 could inhibit mouse spleen cell proliferation induced by concanavalin A (Con A). Molecular docking simulation further elucidated the specific DC838 binding to CypA at the atomic level. The current work should provide useful information in the discovery of immunosuppressor based on CypA inhibitor.

© 2006 Elsevier Ltd. All rights reserved.

## 1. Introduction

Cyclophilin A (CypA) belongs to a soluble cytoplasmic immunophilin, which catalyzes the *cis*–*trans* isomerization of peptidyl-prolyl bonds and acts as molecular chaperone to play assisting role in the protein folding, assembly, and transportation processes.<sup>1,2</sup> CypA could also serve as an intracellular receptor functioning in cell life. Like other immunophilins, CypA has a high binding affinity to the immunosuppressor cyclosporin A (CsA), and CsA inhibits peptidyl-prolyl *cis*–*trans* isomerase activity of CypA.<sup>3,4</sup>

CypA is widely distributed in various tissues, and expressed in highest concentration in the brain.<sup>5</sup> This makes it important in the maturation and folding of neuron-specific proteins in vivo, even though the details of its functional mechanisms are largely unknown. It is reported that CsA can regulate the level of CypA in both undifferentiated and cAMP-induced differentiated murine neuroblastoma (NB) cells in culture.<sup>6</sup> When treated with CsA, the NB cell can partially differentiate into neurons, which implicates a role for CypA in neuronal differentiation.<sup>6</sup> Therefore, CypA ligands might hold great potential for the treatment of nerve injuries and neurological disease.

CsA is a natural fungal cyclic undecapeptide metabolite and has been used as an immunosuppressant drug for the prevention of organ rejection after transplant operations.<sup>7</sup> The CsA-induced immunosuppression has been tentatively explained and related to CypA. It is believed

**Keywords:** Cyclophilin A; Inhibitor; Quinoxaline; Surface plasmon resonance; Fluorescence titration.

\* Corresponding authors. Tel./fax: +86 21 50806918 (X.S.); e-mail addresses: [xshen@mail.shnc.ac.cn](mailto:xshen@mail.shnc.ac.cn); [hljiang@mail.shnc.ac.cn](mailto:hljiang@mail.shnc.ac.cn)

† These authors contributed equally to this work.

that the immunosuppressive action is exercised by the ternary complexes, namely the CsA/CypA complex inhibits the calcineurin (CN) activity, which plays a key role in the signal transduction pathway towards the T-cell activation. Inhibition of CN might prevent dephosphorylation of the cytosolic component of the transcription factor, nuclear factor of activated T cell (NFAT), and prevent its movement into the nucleus where it is critical for the production of immunosignaling cytokines, including interleukin 2, thus leading to the suppression of T-cell activation.<sup>8–11</sup>

CypA is also required for the infectious activity of human immunodeficiency virus type 1 (HIV-1).<sup>12–17</sup> The gag of HIV is a polyprotein and cleaved by proteases into several functional proteins: matrix (MA), capsid (CA), nucleocapsid (NC), and small peptides.<sup>18,19</sup> The HIV CA protein is essential for the assembly and infectivity of HIV virions.<sup>16,18,20,21</sup> CypA binds directly to the CA domain of gag, with a CA-CypA stoichiometry of approximately 10:1 per virion.<sup>13,14,22,23</sup> Formation of the CA-CypA complex is competitively inhibited by molecules that bind to the active site of CypA, including CsA and its nonimmunosuppressive analogue SDZ NIM 811.<sup>12,24</sup> This complex formation can also be inhibited by a series of mutations at the N-terminus of CA. Reagents and mutations that inhibit the CA/CypA interaction in vitro also block CypA packaging and HIV-1 replication in culture, demonstrating that this interaction is essential for viral infectivity.<sup>13–15,25</sup>

Recently, we found that the nucleocapsid (N) protein of SARS-CoV binds to human CypA with high affinity, and the equilibrium dissociation ( $K_D$ ) is 100–2700 times higher than the binding affinity of HIV-1 CA to CypA.<sup>26</sup> Sequence alignment and molecular modeling revealed that SARS-CoV N loop Trp302-Pro310 fits into the active site groove of CypA through hydrogen bonding, cation- $\pi$  and  $-\text{CH}\cdots\pi$  hydrogen bonding interactions. This observed SARS-CoV N/CypA interaction might provide a new hint for the understanding of a possible SARS-CoV infection pathway against human cell, and further supply a feasible approach for anti-SARS agent screening.

Taken together, CypA is involved in many diseases and virus invasion, drug discovery efforts have focused on the development of CypA inhibitors for pharmaceutical research. In the current work, we reported a novel quinoxaline derivative, 2,3-di(furan-2-yl)-6-(3-*N,N*-diethylcarbamoyl-piperidino)carbonylamino quinoxaline (DC838, **3**), which was confirmed to be a potent human CypA inhibitor, and in vivo assay results showed its high inhibition activity against mouse spleen cell proliferation. To further elucidate DC838 binding to CypA at the atomic level, molecular docking simulation on CypA/DC838 binding was also well performed. Both the experimental and computational results should provide useful information in the discovery of immunosuppressor targeting CypA, and the discovered active compound DC838 might be used as a possible lead compound for further research.

## 2. Results and discussion

### 2.1. Synthesis of compound DC838

Generally, compound DC838 was prepared according to the synthetic strategy outlined in Scheme 1. 6-Amino-2,3-di(furan-2-yl)quinoxaline (**1**) was obtained according to the literature method.<sup>27</sup> Reaction of (**1**) with triphosgene under nitrogen at room temperature in the presence of triethylamine afforded 2,3-di(furan-2-yl)-6-isocyanatoquinoxaline<sup>28</sup> (**2**). The target compound (**3**, DC838) was synthesized by the reaction of *N,N*-diethylnipecotamide<sup>29</sup> with (**2**). The structure was confirmed with IR, <sup>1</sup>H NMR and MS spectral analyses.

### 2.2. Kinetic analysis of CypA/DC838 binding by surface plasmon resonance

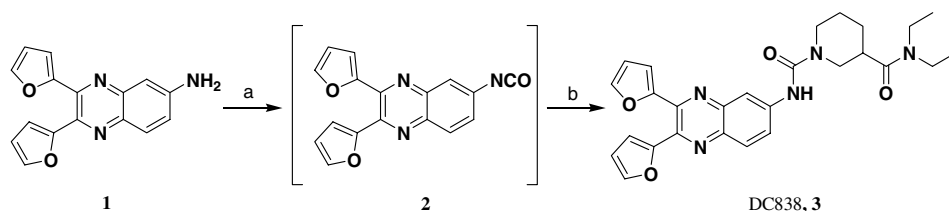
To address the kinetic data of compound DC838 binding to CypA, the SPR technology based Biacore 3000 instrument was used. Immobilization of CypA on the Biacore biosensor chip resulted in a resonance signal of 5370 resonance units (RUs). As shown in Figure 1, the biosensor RUs of DC838 were concentration-dependent, suggesting that DC838 can bind to CypA in vitro. The 1:1 Langmuir binding model was thus used to determine the equilibrium dissociation constant ( $K_D$ ), the association ( $k_{\text{on}}$ ) and dissociation ( $k_{\text{off}}$ ) rate constants by Eqs. 1 and 2.

$$\frac{dR}{dt} = k_{\text{on}} \times C \times (R_{\text{max}} - R) - k_{\text{off}} \times R \quad (1)$$

where  $R$  represents the response unit,  $C$  is the concentration of the analyte, and

$$K_D = k_{\text{off}}/k_{\text{on}} \quad (2)$$

The obtained results were evaluated by  $\chi^2$ , the statistical value in Biacore. All the kinetic parameters are listed in Table 1.



**Scheme 1.** Reagents and conditions: (a)  $(\text{CCl}_3\text{O})_2\text{CO}$ , TEA,  $\text{CH}_2\text{Cl}_2$ , rt, 1 h. (b) *N,N*-diethylnipecotamide, rt, 1 h (72%).

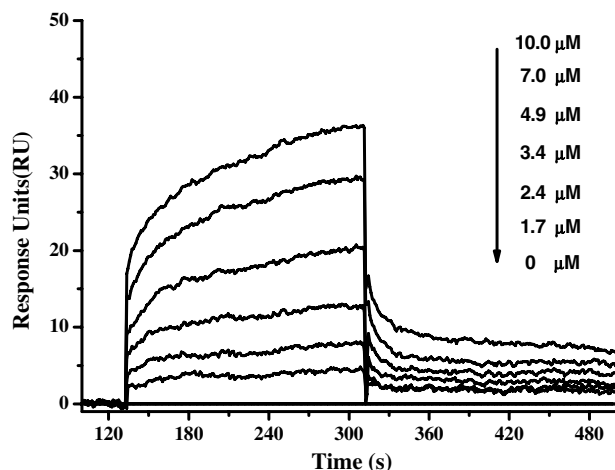


**Figure 1.** Sensorgrams of DC838 binding to CypA measured by SPR. Representative sensorgrams obtained from the injection of DC838 at concentrations of 0, 1.7, 2.4, 3.4, 4.9, 7.0 and 10.0  $\mu\text{M}$  over CypA immobilized on the CM5 chip.

**Table 1.** Kinetic analysis of DC838 binding to CypA evaluated by SPR technology based Biacore 3000

$R_{\text{max}}$ (RU)	$k_{\text{on}}$ (per M per s)	$k_{\text{off}}$ (per s)	$K_{\text{D}}$ ( $\mu\text{M}$ )	$\chi^2$
$36.5 \pm 2.82$	$203 \pm 17.9$	$1.44 \pm 0.022 \times 10^{-3}$	7.09	0.84

$R_{\text{max}}$ , maximum analyte binding capacity;  $k_{\text{on}}$ , association rate constant;  $k_{\text{off}}$ , dissociation rate constant;  $K_{\text{D}}$ , equilibrium dissociation constant.  $K_{\text{D}} = k_{\text{off}}/k_{\text{on}}$ ;  $\chi^2$ , statistical value in Biacore.

The SPR results showed that compound DC838 exhibited strong binding affinity against CypA with  $K_{\text{D}}$  value of 7.09  $\mu\text{M}$ . This  $K_{\text{D}}$  value is found to be in good agreement with the apparent equilibrium dissociation constant ( $K'_{\text{D}}$ ) from the intrinsic fluorescence titration analysis and  $\text{IC}_{50}$  values in the cyclophilin PPIase activity inhibition determination, further suggesting that SPR assay is a powerful and useful method for screening CypA inhibitors.

### 2.3. CypA/DC838 binding analysis by intrinsic fluorescence titration method

As stated in the published results,<sup>30,31</sup> the tryptophan residue (Trp121) around the CypA binding site could be used as an intrinsic probe for studying the interaction between CypA and its ligand. Therefore, we investigated the binding affinity of compound DC838 against CypA by using the published intrinsic fluorescence titration technique.<sup>31</sup> During the assay, a 1:1 stoichiometry of CypA/compound binding was performed according to the published result for CypA/CsA interaction.<sup>32,33</sup> The apparent equilibrium dissociation constant ( $K'_{\text{D}}$ ) for CypA/DC838 binding was thus calculated according to the literature method.<sup>31</sup> It is assumed that 50% occupancy of CypA is set at a fractional fluorescence change of 0.5 ( $\text{FC}_{0.5}$ ), then at this point the concentration of the bound ligand equals to the bound protein, the half of the total concentration of protein. Accordingly,  $K'_{\text{D}}$  is equal to the total ligand concentration at  $\text{FC}_{0.5}$  minus the concentration of the bound protein.<sup>31</sup>

Figure 2 shows the typical tryptophan fluorescence quenching of CypA induced by the titration of DC838 with an increasing concentration. Since compound DC838 itself does not show any intrinsic fluorescence absorption, its possible effect on the experiments could be neglected. Obviously, the evaluated  $K'_{\text{D}}$  value at 3.78  $\mu\text{M}$  is compatible to the  $K_{\text{D}}$  value by Biacore 3000. Moreover, as indicated in Figure 2 and Table 2, the fact that DC838 can perturb CsA binding to CypA during the competition assay by shifting the  $K'_{\text{D}}$  to 10.05  $\mu\text{M}$  for CypA binding to CsA implicates that both DC838 and CsA bind to CypA in the same binding pocket. This is in agreement with the molecular docking analysis result of this work, as will be discussed below.

### 2.4. CypA peptidyl prolyl *cis-trans* isomerase (PPIase) activity inhibition assay

Since CypA belongs to the family of peptidyl prolyl *cis-trans* isomerase (PPIase), the classic spectrophotometric method<sup>34</sup> could be used to determine the PPIase inhibition activity of the tested compound against CypA. During the assay, the rate constants for the *cis-trans* interconversion were evaluated by fitting the data to the integrated first-order rate equation through nonlinear least-square analysis.<sup>34,35</sup> CsA was tested as a positive control for assay assessment, in which the  $\text{IC}_{50}$  of CsA against CypA was figured out as 61.4 nM (Fig. 3), which is in agreement with the previous result.<sup>4</sup>

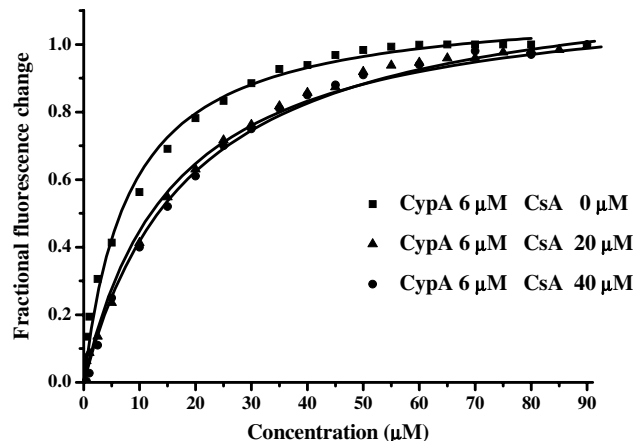


**Figure 2.** Tryptophan fluorescence quenching by compound (DC838) and CsA with DC838 binding to CypA. ■, CypA (6  $\mu\text{M}$ ) was incubated with increasing amounts of DC838 (0–90  $\mu\text{M}$ ); ▲, CypA (6  $\mu\text{M}$ ) with CsA (20  $\mu\text{M}$ ) was incubated with increasing amounts of DC838 (0–90  $\mu\text{M}$ ); ●, CypA (6  $\mu\text{M}$ ) with CsA (40  $\mu\text{M}$ ) was incubated with increasing amounts of DC838 (0–90  $\mu\text{M}$ ). The resulting fluorescence change is plotted as a fraction of the maximal change.

**Table 2.** Apparent equilibrium dissociation constants ( $K_{\text{D}}$ s) of DC838 binding to CypA evaluated by the tryptophan fluorescence quenching method

Compounds	50% occupancy conc ( $\mu\text{M}$ )	$K_{\text{D}}$ ( $\mu\text{M}$ )
DC838 (6 $\mu\text{M}$ )	6.78	3.78
DC838 (6 $\mu\text{M}$ ) + CsA (20 $\mu\text{M}$ )	13.22	10.22
DC838 (6 $\mu\text{M}$ ) + CsA (40 $\mu\text{M}$ )	13.05	10.05

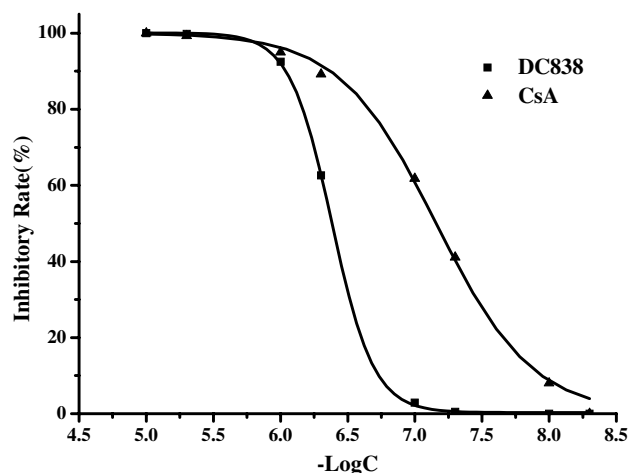


**Figure 3.** CypA PPIase activity inhibition assay for DC838 and CsA. PPIase (25 nM) was pre-incubated with the tested compound at different concentrations, and the PPIase activity change was plotted as a fraction of the maximal change. ▲, CsA (0.005, 0.01, 0.05, 0.1, 0.5, 1, 5, 10  $\mu$ M); ■, DC838 (0.005, 0.01, 0.05, 0.1, 0.5, 1, 5, 10  $\mu$ M). Data are means of 3 independent experiments. Half-maximal inhibitor concentrations ( $IC_{50}$  values) are obtained by sigmoidal fit of inhibitory curves using Origin 7.0.

The inhibition result for the compound DC838 against CypA PPIase activity in a series of concentrations was demonstrated in Figure 3, the  $IC_{50}$  value was thus determined as 0.41  $\mu$ M, which is comparable with the Biacore and fluorescence titration analytical results (Tables 1 and 2). These results thereby further imply the reliability of these three detection approaches.

## 2.5. Inhibition activity of DC838 against the proliferation of the mouse spleen cells

To test the immunosuppressive effects of DC838, the anti-proliferation activity on the mouse spleen cells of this compound has been determined. During the assay, CsA was used as a control for evaluation of DC838 inhibition activity. As demonstrated in Figure 4, the inhibition of the proliferation of spleen cells results with the increase of the compound concentration, and the  $IC_{50}$  values of CsA and DC838 were found to be 1.03  $\mu$ M and 4.32  $\mu$ M, respectively.

To investigate the possible compound toxicity for CsA and DC838 against the spleen cell, the effects on the cell caused by the treatment for 72 h with CsA or DC838 at 100  $\mu$ M and 10  $\mu$ M were assayed (0.106 and 0.113 in  $OD_{540}$  at 100  $\mu$ M to 10  $\mu$ M of CsA against 0.173 for medium,  $P < 0.01$ ; 0.136 in  $OD_{540}$  at 100  $\mu$ M of DC838 against 0.173 for medium,  $P < 0.05$ ). It is noticed that the treatments with CsA both at 100  $\mu$ M and 10  $\mu$ M and DC838 at only 100  $\mu$ M show significant influences on the viability of the naive spleen cells, while at 10  $\mu$ M DC838 shows no apparent influence on the cell viability (data not shown). These results thereby imply that the cytotoxicity of DC838 is probably less than that of CsA, and DC838 might be used as a possible lead compound for further immunosuppressive agent discovery.

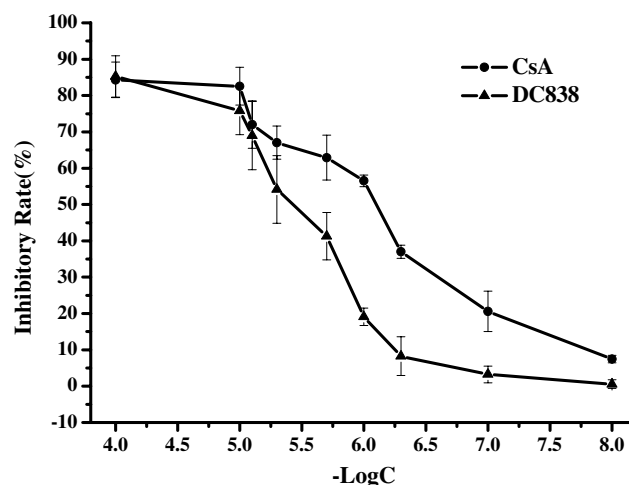


**Figure 4.** DC838 could inhibit the mouse spleen cell proliferation dose-dependently. Spleen cells isolated from naive mice were cultured with 5  $\mu$ g /mL of Con A for 72 h in the presence of increasing concentration of compounds: ●, CsA (0.01, 0.1, 0.5, 1, 2, 5, 8, 10, 100  $\mu$ M); ▲, DC838 (0.01, 0.1, 0.5, 1, 2, 5, 8, 10, 100  $\mu$ M). After culture, MTT assay was used for measuring the cell viability. Each value indicates the mean  $\pm$  SD of three experiments using 3 mice with triplicate sets in each assay. Half-maximal inhibitor concentrations ( $IC_{50}$  values) are obtained by log-probit analysis of inhibitory curves using SPSS, a Windows statistical software package.

## 2.6. Molecular docking analyses

To gain further insight into the CypA/DC838 interaction model at the atomic level, the docking simulation on CypA/DC838 binding was carried out using human CypA crystal structure (PDB entry 1NMK) as the model. The binding pocket of CypA was fairly big and shallow, composed of residues Arg55, Phe60, Met61, Gln63, Gly72, Ala101, Asn102, Ala103, Gln111, Phe113, Trp121, Leu122 and His126. The molecular docking results indicate that DC838 binds into the active site groove of CypA similar to CsA.<sup>33</sup> Different from the case of the full occupation by CsA, DC838 took only partly the binding pocket and might swing in the pocket. The DC838 binding model to CypA was shown in Figure 5. It is found that the carbamoyl forms three hydrogen bonds to CypA: the carbonyl O atom forms two hydrogen bonds with the  $N^{H2}$  atoms of Gln63 and Gln111, respectively, and the N atom hydrogen bonds to the carbonyl O atom of Asn102. The O atom of one furan ring forms a hydrogen bond with the  $-N^{H1}-H$  group of Arg55; and the other furan ring interacts with the benzene ring of Phe113 via  $\pi \cdots \pi$  stacking. The quinoxaline ring forms a  $-NH \cdots \pi$  hydrogen bond with the  $-N^{H1}-H$  group of Arg55. Helekar ever demonstrated that Arg55 of CypA was a key determinant against the PPIase activity.<sup>36</sup> DC838 showed its hydrophobic contacts with Arg55 of CypA. Therefore, the PPIase activity of CypA might be inhibited by the hydrophobic interaction from the inhibitor. In addition, DC838 formed stacking interactions with the only tryptophan residue Trp121 of CypA for contributing to the change of fluorescence intensity (data not shown).

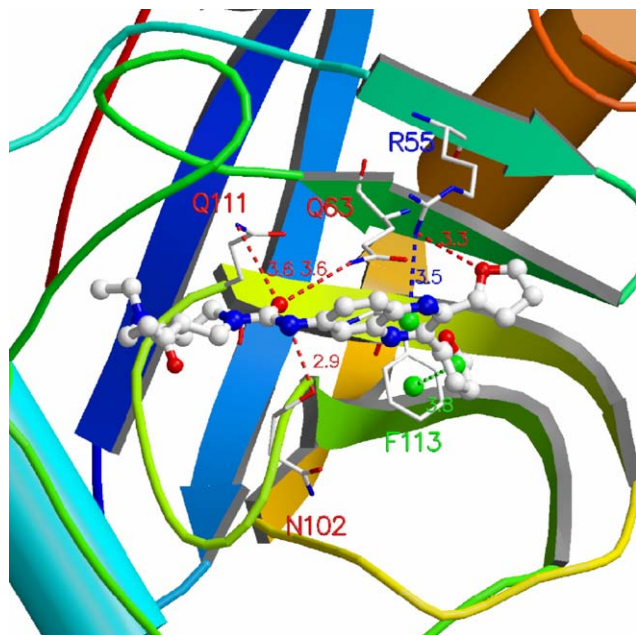


**Figure 5.** Binding model of DC838 to CypA. The structure of DC838 is shown as ball-and-stick model. Red dot lines represent the hydrogen bonds formed between DC838 and CypA, the blue line indicates the  $-NH \cdots \pi$  hydrogen bond, and the green line represents the  $\pi \cdots \pi$  stacking interaction.

### 3. Conclusions

In this work, we report one small molecule quinoxaline derivative DC838 as a novel CypA inhibitor. *In vivo* assays indicated that this compound inhibits mouse spleen cell proliferation induced by concanavalin A. By using SPR and fluorescence titration techniques, kinetic analyses of CypA/DC838 interactions were quantitatively performed. The measured  $IC_{50}$  value for DC838 is in good agreement with the SPR and fluorescence titration results, which suggests that they are powerful approaches for identifying CypA inhibitor. Molecular docking results elucidated the specific binding of DC838 to CypA at the atomic level. The current work should provide useful information in the discovery of immunosuppressor targeting CypA, and DC838 might be used as a lead compound for further research.

## 4. Experimental procedures

### 4.1. Synthesis of DC838

All the reactions were carried out using oven-dried round-bottomed flasks under an atmosphere of nitrogen unless otherwise noted, and the mixture was stirred magnetically. Dichloromethane was distilled from  $CaH_2$ , and triethylamine was distilled from sodium.

IR spectra in KBr disk were obtained on a NicoletMagna IR750; only peaks with wavenumbers greater than  $1200\text{ cm}^{-1}$  are reported.  $^1H$  nuclear magnetic resonance (NMR) spectra (400 MHz) were recorded in  $CDCl_3$  solution on a Bruker AMX-400 instrument.

The preparation of DC838 is depicted in Scheme 1. 6-Amino-2,3-di(furan-2-yl)quinoxaline (**1**) was obtained as described in the literature.<sup>27</sup> Reaction of 6-amino-2,3-di(furan-2-yl)quinoxaline with triphosgene under nitrogen at room temperature in dichloromethane in the present of triethylamine afforded 2,3-di(furan-2-yl)-6-isocyanatoquinoxaline<sup>28</sup> (**2**). *N,N*-Diethylnipecotamide<sup>29</sup> was added into the reaction mixture to afford the target compound (**3**), which was purified by flash chromatography (silica gel, ethyl acetate).

**4.1.1. 6-Amino-2,3-di(furan-2-yl)quinoxaline (1).** The precursor for **1** was synthesized as described by Robert et al.<sup>27</sup>

**4.1.2. 2,3-Di(furan-2-yl)-6-isocyanatoquinoxaline (2).** To a solution of **1** (83.1 mg, 0.30 mmol) and triethylamine (100  $\mu$ L, 0.72 mmol) in dichloromethane (10 mL), was added triphosgene (30 mg, 0.10 mmol) with stirring. The mixture was stirred at room temperature for 1 h, and then used directly for next reaction.

**4.1.3. 2,3-Di(furan-2-yl)-6-(3-*N,N*-diethylcarbamoyl-piperidino)carbonylamino quinoxaline (3).** To the reaction mixture of **2** was added *N,N*-diethylnipecotamide<sup>29</sup> (100 mg, 0.54 mmol, in 2 mL dichloromethane) with stirring at room temperature. The stirring was continued for 1 h. The solvent was evaporated in vacuum to give the crude product. It was purified by flash column chromatography (silica gel, 200–300 mesh) using ethyl acetate as the eluent, giving **3** (105 mg, 72%) as a yellow amorphous solid.  $^1H$  NMR ( $CDCl_3$ , 400 MHz)  $\delta$  7.90–8.02 (m, 4H), 7.58 (m, 2H), 6.60 (d, 1H,  $J = 3.4$  Hz), 6.58 (d, 1H,  $J = 3.4$  Hz), 6.53 (m, 2H), 3.95 (dd, 1H,  $J = 3.3$  Hz, 13.7 Hz), 3.75 (dt, 1H,  $J_d = 4.0$  Hz,  $J_t = 13.2$  Hz), 3.30–3.46 (m, 6H), 2.73 (m, 1H), 1.50–2.00 (m, 4H), 1.22 (t, 3H,  $J = 7.1$  Hz), 1.11 (t, 3H,  $J = 7.1$  Hz); IR (KBr): 3425, 3119, 2933, 2868, 1618, 1570, 1529, 1475, 1429, 1382, 1331, 1256,  $1230\text{ cm}^{-1}$ ; EIMS ( $m/z$ ): 487 ( $M^+$ , 0.77%), 303 (100%), 286, 277, 274, 246, 184, 128, 84, 72; HRMS (EI,  $m/z$ ): calcd for  $C_{27}H_{29}N_5O_4$  ( $M^+$ ) 487.2220, found 487.2227; purity: 95.7% (HPLC, Waters Symmetry  $C_{18}$  column,  $CH_3OH/H_2O = 8:2$ ); 96.9% (HPLC, Waters Nova-Pak  $C_{18}$  column,  $CH_3OH/H_2O = 8:2$ ).

### 4.2. Preparation of His-tagged human CypA protein

All cloning techniques including polymerase chain reaction (PCR), restriction, ligation, *Escherichia coli* transformation, and plasmid DNA preparation were carried out according to the standard methods.<sup>37</sup> The His-tagged CypA protein was expressed and purified from the plasmid pQE30-CypA according to the published procedure.<sup>26</sup>

### 4.3. SPR technology based binding assay

The interaction between compound DC838 and CypA were performed using the dual flow cell Biacore 3000 instrument (Biacore AB, Uppsala, Sweden). All the experiments were carried out using HBS-EP (10 mM *N*-2-hydroxyethylpiperazine-*N'*-2-ethanesulfonic acid

[HEPES], 150 mM NaCl, 3.4 mM EDTA and 0.005% surfactant P20 at pH 7.4) as a running buffer at a constant flow rate of 30  $\mu$ L/min at 25 °C. The protein was immobilized directly and covalently on the hydrophilic carboxymethylated dextran matrix of the CM5 sensor chip (BIAcore) by using the standard primary amine coupling reaction. The protein to be bound to the sensor chip was diluted in 10 mM sodium acetate buffer (pH 6.0) to a concentration of 17  $\mu$ M. The concentrations of the compounds dissolved in the running buffer varied from 1.7 to 10  $\mu$ M. All the data analyses were carried out using BIAevaluation software, and the sensorgrams were processed by automatic correction for nonspecific bulk refractive index effects. The kinetic analyses of the ligand binding to the protein were performed based on the 1:1 Langmuir binding fit model according to the procedures described in the software manual.

#### 4.4. Fluorescence titration assay

Fluorescence measurements were performed on a Hitachi (Tokyo, Japan) F-2500 fluorescence spectrophotometer equipped with a thermal controller. The change in the intrinsic tryptophan fluorescence when the compound bound to the protein (CypA) was monitored using a procedure similar to that described in the literature.<sup>3,31</sup> The experiments were carried out at 25 °C in 20 mM Tris–HCl, 100 mM NaCl (pH 8.0) with the protein concentration set at 6  $\mu$ M and the compound concentrations varied from 0 to 90  $\mu$ M. The compounds were prepared in dimethylsulfoxide (DMSO) as a stock solution of 10 mM. The excitation wavelength was set at 278 nm, the emission range was from 300 nm to 400 nm, and the slit was set at 5 nm. Fluorescence readings were taken at the wavelength of maximum emission, generally 336–346 nm. The resulting fluorescence change conversion as a fraction of maximal change, was plotted versus the total concentration of ligands.

#### 4.5. PPIase inhibition activity assay

CypA PPIase activity was measured at 4 °C by using the standard chymotrypsin-coupled assay.<sup>34</sup> The assay buffer (50 mM HEPES, 100 mM NaCl, pH 8.0) and CypA (500 nM stock solution) were pre-cooled to 4 °C, to which then were added 15  $\mu$ L of 3 mg/mL chymotrypsin in 1 mM HCl. The reaction was initiated by adding 12  $\mu$ L of 3.8 mM peptide substrate (Suc-Ala-Ala-cis-Pro-Phe-pNA) in LiCl/THF solution with rapid inversion. After a delay from the onset of mixing (usually 6 s), the absorbance of *p*-nitroaniline was followed at 390 nm until the reaction was complete (1 min). The final concentration of LiCl in the assay was 9.6 mM; THF was present at a concentration of 2% (v/v). Absorbance readings were collected every 0.1 s by a U-2010 spectrophotometer. The progress curves were analyzed by nonlinear least-squares fit.

The inhibition assays of compounds were performed in the same manner as mentioned above. A 0.6  $\mu$ L aliquot of the compounds in DMSO was added to the CypA

solution in the assay buffer. After pre-incubated for 1 h at 4 °C, the assay was started by the addition of chymotrypsin and the substrate. To calculate the half-maximal inhibitory concentration ( $IC_{50}$ ), percent of remaining PPIase activity was plotted against the common logarithm of the compound concentration, and the data were fitted using the sigmoidal fitting model by the Origin7.0 software.

#### 4.6. Immunological assay

Female ICR strains of mice, 6–8 weeks old and  $20 \pm 2$  g, were purchased from the Experimental Animal House of China Pharmaceutical University (Nanjing, China) and were maintained in plastic cages with free access to pellet food and water (12 h light/dark cycle,  $21 \pm 2$  °C). This study complied with the current ethical regulations on animal research in Nanjing University and the mice used were treated humanely.

The spleen was aseptically taken from mice, crushed gently and separated into single cells by squeezing in 5 mL D-Hank's solution (GIBCO BRL). The cells obtained were passed through eight-layers of gauze and centrifuged at 1000 rev/min for 5 min at 4 °C. Pellets were added into 10 mL of sterile 0.17 M Tris-(hydroxymethyl) aminomethane containing 0.75%  $NH_4Cl$  (pH 7.5) followed by centrifugation to remove erythrocytes. After washing twice with RPMI 1640 containing 100 U/mL of penicillin, 100 U/mL of streptomycin and 10% fetal calf serum (FCS) (RPMI 1640 medium), they were re-suspended in the RPMI 1640 medium and used for cell culture.

Spleen cells were cultured in 96-well flat-bottomed microplates (Falcon) at a density of  $5 \times 10^5$  cells/well in RPMI 1640 medium (0.2 mL) and stimulated with 5  $\mu$ g/mL of ConA for 72 h at 37 °C in 5%  $CO_2$ -air in the presence or absence (control group) of various concentrations of compounds. Then the cell growth was evaluated with modified MTT assay.<sup>38</sup> Briefly, 20  $\mu$ L of 5 mg/mL MTT in RPMI 1640 were added for a further 4 h incubation. After removing the supernatant, 200  $\mu$ L of DMSO were added to dissolve the formazan crystals. The plate was shaken for 10 min, and then read on an ELISA reader (Sunrise Remote/Touch Screen; TECAN, Austria) at 540 nm. All assays were run in triplicate and the effect of compounds on the proliferation of mouse spleen cells induced by Con A was calculated by Eq. 3:

$$\text{Inhibitory rate (\%)} = \frac{(\text{control (OD}_{540}) - \text{compounds (OD}_{540}))}{\text{control (OD}_{540})} \quad (3)$$

Data were expressed as mean  $\pm$  SD (significance of differences between groups). Statistical analysis was evaluated by one-way analysis of variance, followed by Student's two-tailed *t*-test for the evaluation of the difference between two groups and Dunnett's *t*-test between control group and multiple dose groups. One-way analysis of variance revealed a significant effect at  $P < 0.05$ .

#### 4.7. Molecular modeling and docking

The crystal structure of CypA in complex with sanglifehrin macrolide (SFM) (PDB entry 1NMK)<sup>39</sup> recovered from Protein Data Bank (<http://www.rcsb.org/pdb>) was used as a target for molecular modeling and docking. The three dimensional (3D) structure of the compound DC838 was constructed from scratch by Sybyl 6.8,<sup>40</sup> and optimized to energy convergence with the Tripos force field and MMFF94 charges. In the present study, the DOCK4.0 program<sup>41</sup> was employed for the primary molecular docking. Residues of CypA around SFM at a radius of 6.5 Å were isolated for constructing the grids of the docking calculation. The resulting substructure included all residues of the binding pocket. During the docking calculation, Kollman-all-atom charges<sup>42</sup> were assigned to the protein, and Gasteiger–Marsili partial charges<sup>43</sup> were assigned to the small molecule. The surface structure of the binding pocket was constructed by using the MOLCAD module of Sybyl 6.8.

The DOCK suite of programs is designed to find possible orientations of a ligand in a 'receptor' site.<sup>41</sup> The orientation of a ligand is evaluated with a shape-scoring function and/or a function approximating the ligand/receptor binding energy. The shape-scoring function is an empirical function resembling the van der Waals' attractive energy. The ligand/receptor binding energy is taken to be approximately the sum of the van der Waals' and electrostatic interaction energies. After the initial orientation and scoring evaluation, a grid-based rigid body minimization was carried out for the ligand to locate the nearest local energy minimum within the receptor binding site. The position and conformation of each docked molecule were optimized using the single anchor search and torsion minimization method of DOCK 4.0. Thirty conformations per ligand building a cycle and 50 maximum anchor orientations were used in the anchor-first docking algorithm. All docked configurations were energy minimized using 100 maximum iterations and one minimization cycle.

#### Acknowledgments

This work was supported by the State Key Program of Basic Research of China (Grants 2002CB512807, 2004CB58905), the National Natural Science Foundation of China (Grants 30525024, 20372069, 20472095), Shanghai Basic Research Project from the Shanghai Science and Technology Commission (Grants 03DZ19228 and 03DZ19212).

#### References and notes

- Fischer, G.; Wittmann-Liebold, B.; Lang, K.; Kiefhaber, T.; Schmid, F. X. *Nature* **1989**, *337*, 476–478.
- Takahashi, N.; Hayano, T.; Suzuki, M. *Nature* **1989**, *337*, 473–475.
- Handschumacher, R. E.; Harding, M. W.; Rice, J.; Drurge, R. J.; Speicher, D. W. *Science* **1984**, *226*, 544–547.
- Liu, J.; Albers, M. W.; Chen, C. M.; Schreiber, S. L.; Walsh, C. T. *Proc. Natl. Acad. Sci. U.S.A.* **1990**, *87*, 2304–2308.
- Goldner, F. M.; Patrick, J. W. *J. Comp. Neurol.* **1996**, *372*, 283–293.
- Hovland, A. R.; La Rosa, F. G.; Hovland, P. G.; Cole, W. C.; Kumar, A.; Prasad, J. E.; Prasad, K. N. *Neurochem. Int.* **1999**, *35*, 229–235.
- Beveridge, T.; Calne, R. Y. *Transplantation* **1995**, *59*, 1568–1570.
- McCaffrey, P. G.; Luo, C.; Kerppola, T. K.; Jain, J.; Badalian, T. M.; Ho, A. M.; Burgeon, E.; Lane, W. S.; Lambert, J. N.; Curran, T.; Verdine, G. L.; Rao, A.; Hogan, P. G. *Science* **1993**, *262*, 750–754.
- Clipstone, N. A.; Crabtree, G. R. *Nature* **1992**, *357*, 695–697.
- Jain, J.; McCaffrey, P. G.; Miner, Z.; Kerppola, T. K.; Lambert, J. N.; Verdine, G. L.; Curran, T.; Rao, A. *Nature* **1993**, *365*, 352–355.
- Loh, C.; Shaw, K. T.; Carew, J.; Viola, J. P.; Luo, C.; Perrino, B. A.; Rao, A. *J. Biol. Chem.* **1996**, *271*, 10884–10891.
- Luban, J.; Bossolt, K. L.; Franke, E. K.; Kalpana, G. V.; Goff, S. P. *Cell* **1993**, *73*, 1067–1078.
- Franke, E. K.; Yuan, H. E.; Luban, J. *Nature* **1994**, *372*, 359–362.
- Thali, M.; Bukovsky, A.; Kondo, E.; Rosenwirth, B.; Walsh, C., et al. *Nature* **1994**, *372*, 363–365.
- Braaten, D.; Franke, E. K.; Luban, J. *J. Virol.* **1996**, *70*, 4220–4227.
- Freed, E. O. *Virology* **1998**, *251*, 1–15.
- Braaten, D.; Luban, J. *EMBO J.* **2001**, *20*, 1300–1309.
- Wills, J. W.; Craven, R. C. *AIDS* **1991**, *5*, 639–654.
- Gelderblom, H. R. *AIDS* **1991**, *5*, 617–637.
- Braaten, D.; Ansari, H.; Luban, J. *J. Virol.* **1997**, *71*, 2107–2113.
- Dorfman, T.; Weimann, A.; Borsetti, A.; Walsh, C. T.; Gottlinger, H. G. *J. Virol.* **1997**, *71*, 7110–7113.
- Franke, E. K.; Luban, J. *Adv. Exp. Med. Biol.* **1995**, *374*, 217–228.
- Ott, D. E.; Coren, L. V.; Johnson, D. G.; Sowder, R. C.; Arthur, L. O.; Henderson, L. E. *AIDS Res. Hum. Retroviruses* **1995**, *11*, 1003–1006.
- Billich, A.; Hammerschmid, F.; Peichl, P.; Wenger, R.; Zenke, G.; Quesniaux, V.; Rosenwirth, B. *J. Virol.* **1995**, *69*, 2451–2461.
- Steinkasserer, A.; Harrison, R.; Billich, A.; Hammerschmid, F.; Werner, G.; Wolff, B.; Peichl, P.; Palfi, G.; Schnitzel, W.; Mlynar, E. *J. Virol.* **1995**, *69*, 814–824.
- Luo, C.; Luo, H. B., et al. *Biochem. Biophys. Res. Commun.* **2004**, *321*, 557–565.
- Alaimo, R. J. US 4,540,693, 1985.
- Collman, J. P.; Wang, Z.; Straumanis, A. *J. Org. Chem.* **1998**, *63*, 2424–2425.
- Zheng, X.; Day, C.; Gollamudi, R. *Chirality* **1995**, *7*, 90–95.
- Liu, J.; Chen, C. M.; Walsh, C. T. *Biochemistry* **1991**, *30*, 2306–2310.
- Husi, H.; Zurini, M. G. *Anal. Biochem.* **1994**, *222*, 251–255.
- Kallen, J.; Spitzfaden, C.; Zurini, M. G.; Wider, G.; Widmer, H.; Wuthrich, K., et al. *Nature* **1991**, *353*, 276–279.
- Pflugl, G.; Kallen, J.; Schirmer, T.; Jansonius, J. N.; Zurini, M. G.; Walkinshaw, M. D., et al. *Nature* **1993**, *361*, 91–94.
- Kofron, J. L.; Kuzmic, P.; Kishore, V.; Colon-Bonilla, E.; Rich, D. H. *Biochemistry* **1991**, *30*, 6127–6134.
- Fischer, G.; Berger, E.; Bang, H. *FEBS Lett.* **1989**, *250*, 267–270.

36. Helekar, S. A.; Patrick, J. *Proc. Natl. Acad. Sci. U.S.A.* **1997**, *94*, 5432–5437.
37. Sambrook, J.; Fritsch, E. F.; Maniatis, T. *Molecular Cloning: A Laboratory Manual*, 2nd ed.; Cold Spring Harbor Laboratory: New York, USA, 1989.
38. Sargent, J. M.; Taylor, C. G. *Br. J. Cancer* **1989**, *60*, 206–210.
39. Sedrani, R.; Kallen, J., et al. *J. Am. Chem. Soc.* **2003**, *125*, 3849–3859.
40. Sybyl [molecular modeling package]. St. Louis, MO: Tripos Associates; 2000.
41. Ewing, T. J. A.; Kuntz, I. D. *J. Comput. Chem.* **1997**, *18*, 1175–1189.
42. Weiner, S. J.; Kollman, P. A.; Nguyen, D. T.; Case, D. A. *J. Comput. Chem.* **1986**, *7*, 230–252.
43. Gasteiger, J.; Marsili, M. *Tetrahedron* **1980**, *36*, 3219–3228.